ACS APPLIED MATERIALS & INTERFACES

Research Article

www.acsami.org

Composite Microdiscs with a Magnetic Belt: Preparation, Chaining Properties, and Use as Switchable Catalyst Carriers

Matti Knaapila,*[,†,‡] Henrik Høyer,[§] and Geir Helgesen[†,∥]

[†]Physics Department, Institute for Energy Technology, NO-2027 Kjeller, Norway

[‡]Department of Physics, Technical University of Denmark, DK-2800 Kongens Lyngby, Denmark

[§]GIAMAG Technologies AS, NO-2027 Kjeller, Norway

[∥]Department of Physics, University of Oslo, NO-0316 Oslo, Norway

ABSTRACT: We describe an emulsion-based preparation of patchy composite particles (diameter of 100−500 μm) consisting of a disclike epoxy core and a belt of porous polystyrene particles (diameter of 30 μm) with magnetite within the pores. Compared to the magnetically uniform polystyrene particles, the spontaneous aggregation of composite particles is suppressed when dispersed into liquid, which is attributed to the increased particle size, reduced magnetic susceptibility, and the shape of the magnetic domain distribution within the particles (spherical versus a belt). When the composite particles are coated by platinum−palladium layer we demonstrate they can be employed as switchable catalyst carriers, moving from one liquid phase to another when controlled by an external magnetic field.

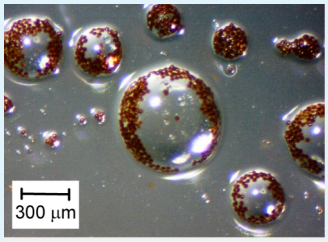

KEYWORDS: *magnetic particles, patchy particles, hybrid materials, active materials, anisotropy, catalyst*

INTRODUCTION

Magnetic field-responsive polymer composites[1,2] containing submicron- or micron-sized ferri- or ferromagnetic particles dispersed in a polymer matrix have a rich variety of applications including actuators[3,4] and magnetorheological elastomers.[5,6] These composites can be produced as microparticles with two notable properties. First, they can incorporate different functionalities having, for example, a magnetic core connected to a polymer shell with a catalytically active palladium group.[7] Polymer coiling and thus catalytic activity can be controlled through thermal transition, while the magnetic core allows magnetic separation and the reuse of the catalyst. Second, they can show anisotropy locally within the particles (1) or globally among the particles aligned within the matrix as induced by (2) external or (3) internal fields.

(1) The particles can manifest internal magnetic anisotropy. Micron-sized polymer particles with permanent internal magnetic anisotropy, also known as magnetic Janus particles, can be prepared from the mixture of oligomers and magnetic beads using microfluidics combined with an external magnetic field upon polymerization.[8] This method has numerous variants including addition of nonmagnetic colloidal beads that are accumulated onto the particle-end opposite the magnetic beads driven by magnetic and gravitational forces[9] or by chemical functionalization of the particle itself.[10] An alternative method is to use microfluidics for particle formation and mix magnetic beads or magnetic nanoparticles with two different polymers and a selective solvent, the solvent evaporation leading to phase segregation and bead accumulation into one phase.[11,12]

Particles may also be half-immersed into a soft polymer matrix such that the magnetic beads are transferred onto the surface of the nonimmersed half by chemical vapor deposition.[13] Detaching these half-coated particles from the polymer substrate produces asymmetric Janus particles and, with an extra etching step, ternary particles with a belt around the particles. Common to these methods are exceedingly well-defined monodisperse particles but certain difficulties in scaling up of the process for potential bulk applications.

(2) The particles can be assembled and aligned into chainlike formations by an external magnetic field. Aligning particles by external field allows anisotropic conductivity,[14,15] magnetic susceptibility,[16] permittivity,[17] magnetoresitance,[18] or piezoresistivity.[14,19] Aligning particle chain from an isotropic dilute system also leads to a conductivity jump and increased transparency in the alignment direction.[20,21]

(3) When dispersed into a fluid, the particles can interact through magnetic dipolar forces and self-organize into anisotropic aggregates even without an external field. This process is diffusion-limited and depends on magnetic moments that in turn depend on the particle size and composition.[22,23]

In this paper, we describe emulsion-based preparation of composite particles (diameter of 100−500 μm) consisting of a disclike epoxy core and a belt of porous PS particles (diameter of 30 μm) with magnetite within the pores. Compared to the relatively uniform polystyrene (PS) particles, the spontaneous aggregation of composite particles is suppressed when dispersed into a liquid, which is attributed to the increased particle size, smaller relative magnetic susceptibility, and the shape of the magnetic domain (sphere versus belt). When the composite particles are coated by a platinum−palladium layer

Received: February 4, 2015
Accepted: March 23, 2015
Published: March 23, 2015

DOI: 10.1021/acsami.5b01053
ACS Appl. Mater. Interfaces 2015, 7, 7795−7800

we demonstrate that they can be employed as switchable catalyst carriers, controlled by an external magnetic field. While this simple idea does not allow the formation of monodisperse and magnetically homogeneous composite particles, it allows a route toward mass-producing composite particles and could be followed by standard roll-to-roll and printing methods.

THEORY

Particle Aggregation. When paramagnetic microparticles are exposed to an external field, they form chains due to the induced dipole−dipole interaction with energy

$$U_{dd} = \frac{\mu_0}{4\pi} \cdot \frac{m^2[1 - 3(\cos\theta)^2]}{r^2} \quad (1)$$

where m is the induced magnetic moment, r is the center-to-center distance of a pair of microparticles, μ_0 is the permeability of free space, and θ is the angle between the directions of their magnetic moments and the line joining the particle centers. Here, $m = \pi d^3 \rho \chi B/6 \mu_0$ where d is the particle diameter, χ is their magnetic susceptibility, and B is the magnetic flux density. For stronger external fields, the particles tend to align their relative positions with the field lines, that is, $\theta = 0$.

The strength of the pairwise magnetic interactions acting in such a system relative to thermal forces (Brownian diffusion) can be characterized by the dipole coupling parameter[22]

$$K_{dd} = \frac{|U_{dd}|}{k_B T} \quad (2)$$

at contact, that is, for $r = d$. Here k_B is Boltzmann's constant and T is the temperature.

The single-particle energy in a magnetic field of flux density $\mathbf{B}$ is

$$U_{df} = -\mathbf{m}\cdot\mathbf{B} \quad (3)$$

From this expression it can be deduced that the magnetic force pulling a magnetic particle exposed to a flux density $\mathbf{B}$ is generally given by[24]

$$\mathbf{F_m} = \frac{1}{\mu_0}\chi V(\mathbf{B}\cdot\nabla)\mathbf{B} \quad (4)$$

where μ_0 is the permeability of free space and V is the particle volume. Thus, the force depends on both the flux density and its gradient $\nabla\mathbf{B}$.

The single-particle effect of the magnetic field is characterized by the field coupling parameter[22]

$$K_{df} = \frac{|U_{df}|}{k_B T} \quad (5)$$

For $K_{dd} \gg 1$ and $K_{df} \gg 1$, the magnetic forces dominate over diffusion effects. For $K_{dd} \ll K_{df}$ the effect of external field in aligning particles into linear chains dominates over the magnetic dipole−dipole aggregation forming branched particle structures.

The magnetic Bjerrum length, that is, the length over which magnetic forces are significant relative to thermal effects, can be defined as[25]

$$\lambda_B = \sqrt[3]{\frac{\mu_0 m^2}{2\pi k_B T}} \quad (6)$$

Particle Trapped at Liquid−Liquid Interface. The energy needed to remove a spherical particle of diameter d trapped at an interface of interfacial tension γ_{12} between liquid 1 and liquid 2 can be written as[26]

$$E = \frac{\pi}{4} d^2 \gamma_{12}(1 + \cos(\theta))^2 \quad (7)$$

where d is the particle diameter and θ is the contact angle, that is, the angle between the interface and the tangent to the particle surface at the contact point. The maximum energy needed to remove any particle from the interface is then

$$E = 2\pi d^2 \gamma_{12} \quad (8)$$

The force F needed to pull a spherical particle through the interface can be estimated to be of the order

$$F \approx E/d \quad (9)$$

EXPERIMENTAL SECTION

Materials. The magnetic microparticles used in the experiments were porous PS particles filled with magnetite (Fe_3O_4) with an Fe content of ∼24%. The particle density was ∼1.7 g/cm^3, and the diameter was 30 μm. The particles were provided as a dry powder by SINTEF (Norway). The matrix of composite particles was made of a two-component low-viscosity oligomer mixture that consisted of Araldite AY 105−1 (Huntsman Advanced Materials GmbH) and Ren HY 5160 (Vantico AG) hardener. The epoxy resin was based on 4,4′-isopropylidenediphenol with the density of ∼1.2 g/cm^3. The hardener contained 50−60% polyoxypropylenediamine, 14−20% benzylalcohol, 10−18% isophorondiamine, and 1−5% trimethylhexamethylenediamine. Both were supplied by Lindberg & Lund AS (Norway). The mixing ratio of the epoxy over the hardener was 2:1 parts per weight. Silicone oil Baysilone containing α-(trimethylsilyl)-ω-(trimethylsilyloxy)polydimethylsiloxane was purchased from Sigma-Aldrich. The viscosity was 1000 mPa·s, and density was 0.97 g/cm^3. Anhydrous toluene (99.8%, viscosity of 0.59 mPa·s and density of 0.87 g/cm^3) was purchased from Sigma-Aldrich, and Perhydrol hydrogen peroxide (30%) was purchased from Merck KGaA (viscosity 1.25 mPa·s, density 1.45 g/cm^3).

Instrumentation. Pt/Pd coating was done using a Cressington 208HR sputter coater with Cressington MTM-20 thickness controller and 0.1 mm thick Pt/Pd target (No. 81006). Optical micrographs were taken using a Motic SMZ-161 stereomicroscope.

External magnetic fields were created by a Halbach cylinder consisting of 12 separate NdFeB N52-grade magnets designed by GIAMAG Technologies AS (Norway). The cylinder length and internal spacings were 2.5 and 1 cm, respectively. An alternative field was set by a 1 cm long cubelike NdFeB permanent magnet supplied by HKCM-Engineering (Germany).

Magnetic susceptibility (χ_{meas}) was measured by a MS3 Magnetic Susceptibility meter connected to a MS2G Single Frequency Sensor (Barrington Instruments). The obtained susceptibility was an average of 10 separate 5 s measurements. The sample was shaken and rotated 90° between each measurement. Volume and mass susceptibilities (χ and χ_m) were obtained using instrument-specific correction algorithms.

Magnetic field strength was measured using Alphalab Gaussmeter GM2 magnetometer with the standard probe. The measured magnetic flux density $\mathbf{B}$ along the center line inside the Halbach magnet was from 0.95 to 0.8 T when coming from the center to the cylinder exit. The magnetic flux densities for the cubelike magnet were 57 mT and 2 mT at 1 and 5 cm separation from its surface.

Preparation of Composite Microdiscs. Figure 1 illustrates the preparation of the composite particles consisting of magnetite containing PS particles placed within an epoxy matrix. (a) The preparation of these particles was initiated from preparing two initial mixtures. (1) 10% PS particles in silicone oil and (2) an epoxy resin with a hardener. These mixtures were mixed together to form a liquid−liquid emulsion such that the mixture-1 was the matrix and the

DOI: 10.1021/acsami.5b01053
ACS Appl. Mater. Interfaces 2015, 7, 7795−7800

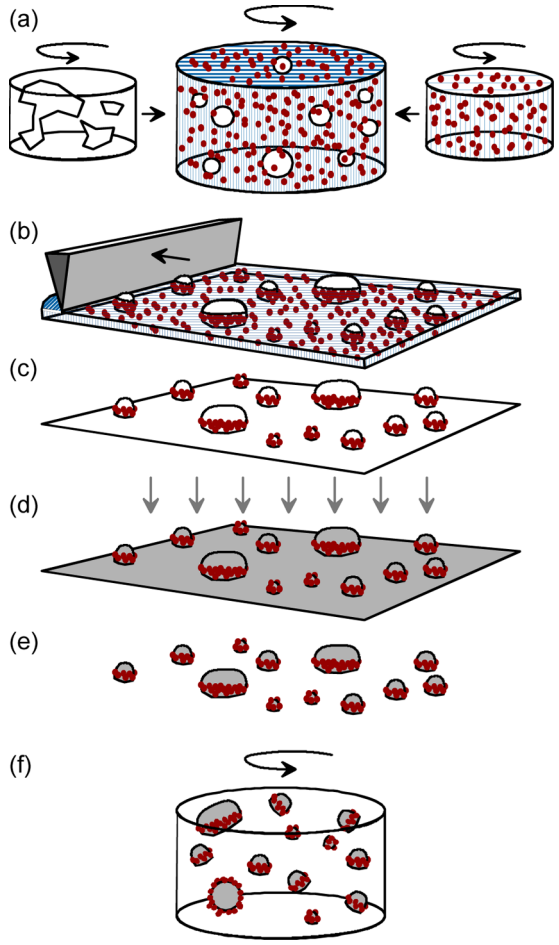

Figure 1. Preparation of patchy composite particles. (a) Forming an emulsion of epoxy resin with a hardener and silicone oil containing magnetic particles. (b) Preparing the emulsion film and the subsequent curing of the drops. The film thickness corresponds to the drop size. (c) Removing the silicon oil matrix. (d) Evaporating a layer of Pt/Pd alloy on the composite particles. (e) Detaching the particles from the surface and (f) dispersing them in toluene.

mixture-2 the minority compound (10−30%). The mixtures are not miscible, but the mixture-2 formed predominantly spherical drops with diameters in the range of 50−500 μm. (b) This emulsion was spread to form an ∼200 μm thick film on a glass surface by the doctor blade method. In this film the largest drops of mixture-2 reach through the thickness of the whole film, and the smaller PS particles tend to accumulate at the interface of these drops. The mixture-2 drops become fully covered by PS particles whenever they are fully immersed in the mixture-1. Since the top part of the drops reach into air above the film and the bottom part touches the substrate, the PS particles tend to form an irregular beltlike ring around the drops. These drops become somewhat flattened during the film formation leading to disclike objects with a patchy PS belt. The microdiscs were cured at room temperature for 6 h, which also binds them to the substrate. (c) The matrix was removed by washing the film with excess toluene and (d) the solid particles were coated by a 50 nm layer of Pt/Pd alloy from the top. (e,f) The final particles were gently removed and dispersed in toluene.

Magnetically Switchable Catalyst Carrier. Hydrogen peroxide decomposes into water and oxygen gas as $2H_2O_2(aq) \rightarrow 2H_2O(l) + O_2(g)$. This reaction is slow, but when catalyzed by platinum it leads to visible oxygen bubble arising from aqueous H_2O_2. This reaction was studied using a small test tube with an aqueous H_2O_2 layer covered by a toluene layer. A part of the composite particles were coated by a layer of Pt/Pd alloy using the sputter-coating as mentioned above. The coated particles were added to this system, and the Halbach magnet was used to move particles between the toluene and hydrogen peroxide phases to start or stop the catalysis.

RESULTS AND DISCUSSION

Figure 2 shows optical micrographs illustrating the preparation of the composite particles. This preparation involves the mixing

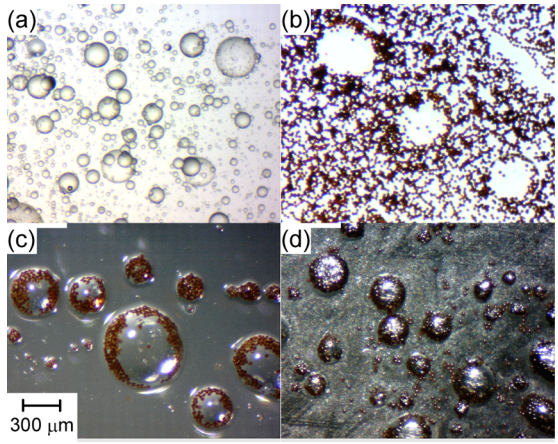

Figure 2. Optical micrographs showing the preparation of composite particles. (a) Bulk emulsion without the PS particles. (b) Emulsion film with the PS particles. (c) Cured microdiscs after matrix removal. (d) Cured particles after Pt/Pd coating.

of two mixtures, one of epoxy resin with a hardener and another of silicone oil with magnetic PS particles. The epoxy phase is the minority compound in the so-obtained emulsion and remains as drops in the silicone phase. The droplet formation is best visible without the red magnetically loaded PS particles (Figure 2a). This emulsion is spread onto a glass substrate to make a film having a thickness (100−300 μm) of the same order of magnitude as the size of epoxy drops (Figure 2b).

The epoxy drops are slightly heavier than silicone oil and tend to fall to the bottom of the film. These drops become semispherical or half-ellipsoidal. Magnetic PS particles tend to accumulate on the surface of the epoxy drops and are locked in placed when the drops are cured. The drops that are slightly larger than the film thickness do not remain flat after the spreading process but slightly contract, pushing the uppermost part of the hemisphere outside the film. In this case, the PS particles do not cover the part outside the film but accumulate only on the sides of the drops forming a continuous belt around the drop. Washing the silicone oil off reveals the composite particles on the surface (Figure 2c). To add an extra functionality, the upper hemispherical part of the composite particles can be subsequently coated by a Pt−Pd layer (Figure 2d).

Figure 3 shows low-oblique images of composite particles on the surface illustrating their disclike shape and the belt of magnetic PS particles. The diameter of PS particles is 30 μm, while the dimensions of composite particles reach from tens to hundreds of micrometers.

Next, we focus on the magnetic properties, spontaneous aggregation, and the chaining of PS particles and composite particles. The susceptibilities of the systems studied are compiled in Table 1. The mass magnetic susceptibility of pure magnetic PS particles is 3×10^{-4} m^3/kg. It scales as the

DOI: 10.1021/acsami.5b01053
ACS Appl. Mater. Interfaces 2015, 7, 7795−7800

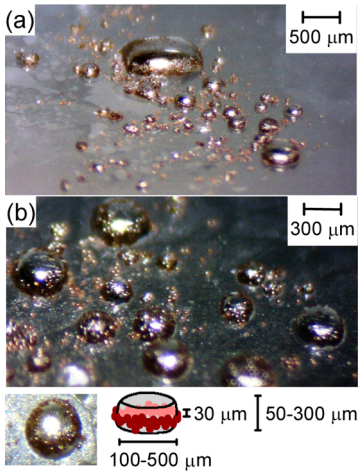

Figure 3. (a, b) Low-oblique micrographs of composite particles illustrating their disclike shapes and magnetic particle belts around the disc sides. (inset) Illustration of typical dimensions of the composite particle.

Table 1. Magnetic Susceptibilities

sample	state	% (w/w)	χ	χ_m (m^3/kg)
magnetic PS particles	solid state	100	~0.5	3.0×10^{-4}
magnetic PS particles	toluene dispersion	0.26	1.1×10^{-3}	
composite particles	toluene dispersion	0.26	1.5×10^{-4}	

magnetite content when the pure PS particles are dispersed in toluene and drops still one order of magnitude for similar dispersion of composite particles. This is plausible since the composite particles contain 10% of PS particles on average.

Figure 4 shows optical micrographs of an ~1 mm thick fluid layer of freely moving PS particles and detached composite particles dispersed in toluene (0.26% (w/w)) without and with an external 2 mT magnetic field. The particles are heavier than toluene and sink to the bottom of the dispersion. The PS particles form a random network structure without external field and chain structures with an external field. The composite particles form loosely bound groups without the field. However, with the external field, composite particles aggregate into asymmetric clusters rather than one-dimensional chains.

The difference in particle behavior shown in Figure 4 can be understood as follows. Considering the magnetic PS particles in toluene, eqs 2 and 5 yield values $K_{dd} \approx 2 \times 10^5$ and $K_{df} \approx 5 \times 10^6$ for the magnet employed in Figure 4. This means that $K_{df} \gg K_{dd} \gg 1$, and the direct forces from the magnet clearly dominate over the diffusion effects. Using eq 6 we estimate a magnetic Bjerrum length of ~2 mm. Thus, the effect of moving and aligning particles along field lines dominates over the tendency of magnetic dipole−dipole aggregation, and linear structures of typical length scale of order 2 mm are expected to form. This is in good agreement with what can be seen for the PS particles in toluene in Figure 4c,e.

Considering the composite particles, eqs 2 and 5 indicate that $K_{dd} \propto d^4$ and $K_{df} \propto d^3$. Thus, when the particle size d increases, K_{dd} grows faster than K_{df}. This means that for large particles dipole−dipole forces are more important than field alignment forces, and alignment in chains along the field is less pronounced for the larger composite particles.

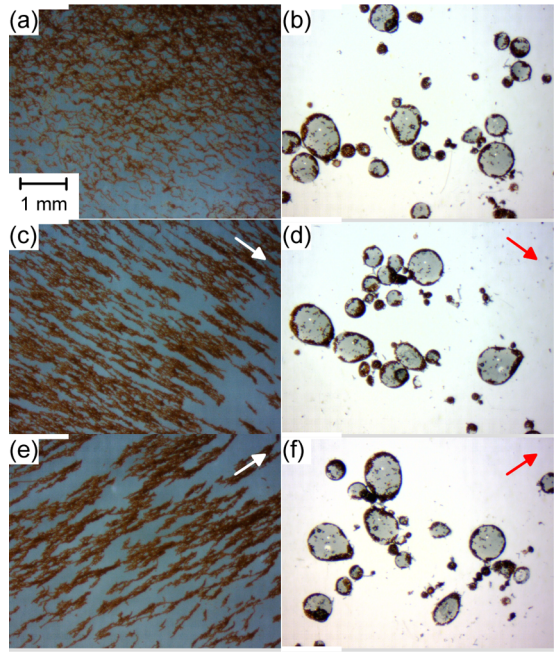

Figure 4. Optical micrographs of freely moving magnetic PS (a, c, e) and composite particles (b, d, f) in a 1 mm thick toluene layer without an external field (a, b) and with an external 2 mT magnetic field toward southeast (c, d) and northeast (e, f). Arrows mark the direction of external fields.

Figure 5 shows optical micrographs of freely moving composite particles in a toluene layer after gently shaking without an external field. The moderate shaking brings particles into the vicinity of other particles, leading to spontaneous aggregation. These aggregates seem not to be destroyed by

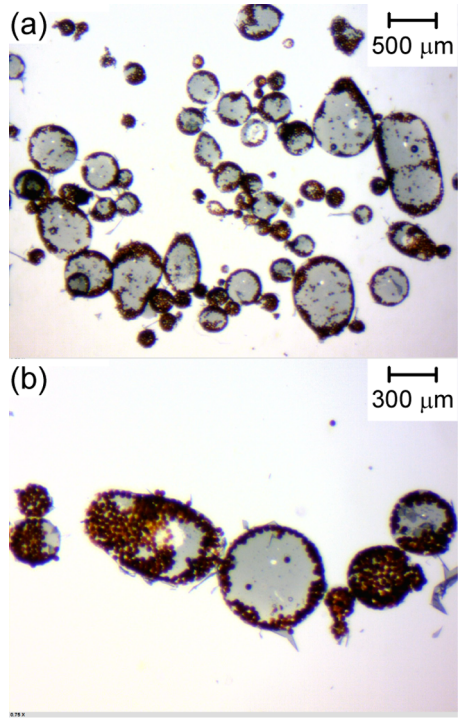

Figure 5. (a, b) Optical micrographs of freely moving composite particles in a 1 mm thick toluene layer after gently shaking without an external magnetic field.

DOI: 10.1021/acsami.5b01053
ACS Appl. Mater. Interfaces 2015, 7, 7795−7800

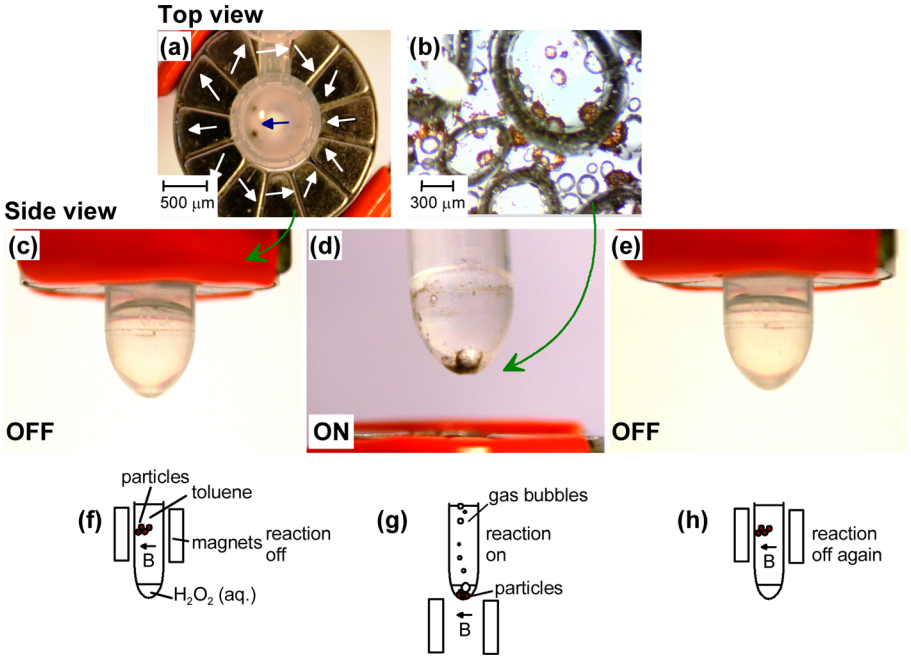

Figure 6. (a) Top view of a test tube that contains composite particles and two solvent layers: H_2O_2(aq) as the lower and toluene as the upper layer. The tube is inserted within the Halbach cylinder. White and blue arrows show the magnetization and the field directions, respectively. (b) A micrograph of gas bubble formation catalysts by the composite particles in the H_2O_2(aq) layer. (c–e) Photos and (f–h) illustration of the mutual arrangement of magnet, composite particles, and solvent layers. The reaction is initiated when particles are dragged from toluene (c) to H_2O_2(aq) layer (d) and suppressed in the subsequent opposite move (e). Green arrows indicate the relation between (a, c) and (b, d).

weakly shaking, and the process yields millimeter sized chainlike agglomerates along the shaking direction. These particles have earlier been exposed to magnetic fields, and spontaneous aggregation implies that the particles may have obtained a small remnant magnetization in the field.

When the force is sufficiently strong, the composite particles can be dragged from one liquid phase into another and back again. A number of studies show how this effect can be used in dragging magnetic catalytic particles from the reaction pool for catalyst recycling.[27] Pt-coated microparticles have been employed as active materials when immersed in aqueous H_2O_2 where platinum catalyzes peroxide dissociation.[28] This reaction is visually observable due to the released oxygen bubbles, which also push particles away.

Figure 6 illustrates behavior of the composite particles in the two-phase system containing toluene (upper phase) and aqueous H_2O_2 (lower phase) within a test tube. The tube is initially placed partly inside the Halbach cylinder such that the toluene phase is inside and the H_2O_2(aq) phase is outside the magnet. The maximum field of the magnet is within this hole, and the field drops quickly outside. The dispersed composite particles are dragged by the field and located in the toluene phase inside the magnet. When the test tube is moved relative to the magnet, the field drags particles into the H_2O_2 phase, catalyzing H_2O_2 dissociation with distinctive bubble formation. When the tube is moved to the initial position, the reaction is stopped.

The process illustrated in Figure 6 can be understood as follows. The interfacial tension for the H_2O_2(aq)–toluene interface is supposedly similar as the interfacial tension for a water–toluene interface, $\gamma_{12} \approx 3.6 \times 10^{-2}$ N/m.[29] From eqs 8 and 9 we estimate that the force needed to pull a $d \approx 300$ μm composite particle through this interface is $F \approx 7 \times 10^{-5}$ N. An external magnet can be used to pull the particle through this interface by a force that depends on the field and the field gradient $\nabla\mathbf{B}$.[30] On the basis of eq 4 we estimate that a lower limit for the magnetic force is $F_m^{min} = (1/\mu_0)\chi V B_z\,(dB_x/dz) \approx 2 \times 10^{-5}$ N, using $B_z \approx 100$ mT and $dB_x/dz \approx 100$ T/m, which were measured just outside the opening of the magnet. The z-direction is along the axis of Halbach cylinder and the x-direction perpendicular to it (the main direction of the field). This value is of the same order of magnitude as the force needed to move a particle through the interface, thus allowing the dragging process.

The dragging of composite particles through H_2O_2(aq)–toluene interface is not possible by applying the cubic magnet used to align the particles as shown in Figure 4. In this case, the field and field gradient are 60 mT and 12 T/m at a separation of 1 cm, corresponding to the thickness of the lower phase in the test tube. This magnet gives rise to a magnetic force of $F_m \approx 1 \times 10^{-6}$ N on our composite particles (eq 4). While this estimation does not take into account details such as particle shape and particle demagnetization effect, it implies that the magnetic force F_m is an order of magnitude smaller than the interfacial force F and thus explains why the dragging is not possible using our cubic magnet.

CONCLUSIONS

In this paper, we describe emulsion-based preparation of composite particles (diameter of 100–500 μm) consisting of a disclike epoxy core and a belt of porous PS particles (diameter of 30 μm) containing magnetite within the pores. Compared to the magnetically uniform PS particles, the spontaneous aggregation of the composite particles is suppressed when dispersed into a liquid, which is attributed to the increased particle size, reduced magnetic susceptibility, and the location of magnetic domains within a belt around the particle. For composite particles coated by a platinum–palladium layer we

DOI: 10.1021/acsami.5b01053
ACS Appl. Mater. Interfaces 2015, 7, 7795–7800

demonstrate that they can be employed as switchable catalyst carriers, moving from one liquid phase to another as controlled by an external magnetic field.

AUTHOR INFORMATION

Corresponding Author

*E-mail: matti.knaapila@fysik.dtu.dk.

Notes

The authors declare no competing financial interest.

ACKNOWLEDGMENTS

We thank T. Furuseth of the Institute for Energy Technology for assistance with sputtering and P. Dommersnes of GIAMAG Technologies and J.-O. Fossum of the Norwegian University of Science and Technology for discussions.

REFERENCES

(1) Filipcsei, G.; Csetneki, I.; Szilagyi, A.; Zrinyi, M. *Adv. Polym. Sci.* **2007**, *206*, 137−189.
(2) Thevenot, J.; Oliveira, H.; Sandre, O.; Lecommandoux, S. *Chem. Soc. Rev.* **2013**, *42*, 7099−7116.
(3) Hosoda, H.; Takeuchi, S.; Inamura, T.; Wakashima, K. *Sci. Technol. Adv. Mater.* **2004**, *5*, 503−509.
(4) Schmidt, A. M. *Macrom. Rapid Commun.* **2006**, *27*, 1168−1172.
(5) Kchit, N.; Bossis, G. *J. Phys. D: Appl. Phys.* **2009**, *42*, 105505.
(6) Kchit, N.; Lancon, P.; Bossis, G. *J. Phys. D: Appl. Phys.* **2009**, *42*, 105506.
(7) Zeltner, M.; Schätz, A.; Hefti, M. L.; Stark, W. J. *J. Mater. Chem.* **2011**, *21*, 2991−2996.
(8) Nguyen, N. T. *Microfluid. Nanofluid.* **2012**, *12*, 1−16.
(9) Chen, Y. H.; Nurumbetov, G.; Chen, R.; Ballard, N.; Bon, S. A. F. *Langmuir* **2013**, *29*, 12657−12662.
(10) Yabu, H.; Ohshima, H.; Saito, Y. *ACS Appl. Mater. Interfaces* **2014**, *6*, 18122−18128.
(11) Jeong, J.; Um, E.; Park, J. K.; Kim, M. W. *RSC Adv.* **2013**, *3*, 11801−11806.
(12) Yabu, H.; Kanahara, M.; Shimomura, M.; Arita, T.; Harano, K.; Nakamura, E.; Higuchi, T.; Jinnai, H. *ACS Appl. Mater. Interfaces* **2013**, *5*, 3262−3266.
(13) Lin, C.-C.; Liao, C.-W.; Chao, Y.-C.; Kuo, C. *ACS Appl. Mater. Interfaces* **2010**, *2*, 3185−3191.
(14) Martin, J. E.; Anderson, R. A.; Odinek, J.; Adolf, D.; Williamson, J. *Phys. Rev. B* **2003**, *67*, 094207.
(15) Yamato, M.; Obayashi, S.; Nishiyama, T.; Horibe, H.; Takahashi, K.; Watanabe, K. *Polymer* **2014**, *55*, 6546−6551.
(16) Martin, J. E.; Venturini, E.; Odinek, J.; Anderson, R. A. *Phys. Rev. E* **2000**, *61*, 2818−2830.
(17) Li, W.; Yu, L.; Zhu, Y.; Hua, D. *J. Phys. Chem. C* **2010**, *114*, 14004−14007.
(18) Mietta, J. L.; Ruiz, M. M.; Antonel, P. S.; Perez, O. E.; Butera, A.; Jorge, G.; Negri, R. M. *Langmuir* **2012**, *28*, 6985−6996.
(19) Khit, N.; Bossis, G. *J. Phys. Condens. Matter* **2008**, *20*, 204136.
(20) Jin, S.; Tiefel, T. H.; Wolfe, R. *IEEE Trans. Magn.* **1992**, *28*, 2211−2213.
(21) Knaapila, M.; Høyer, H.; Kjelstrup-Hansen, J.; Helgesen, G. *ACS Appl. Mater. Interfaces* **2014**, *6*, 3469−3476.
(22) Helgesen, G.; Skjeltorp, A. T.; Mors, P. M.; Botet, R.; Jullien, R. *Phys. Rev. Lett.* **1988**, *61*, 1736−1739.
(23) Tracy, J. B.; Crawford, T. M. *MRS Bull.* **2013**, *38*, 915−920.
(24) Hatch, G. P.; Stelter, R. E. *J. Magn. Magn. Mater.* **2001**, *225*, 262−276.
(25) Faraudo, J.; Andreu, J. S.; Camacho, J. *Soft Matter* **2013**, *9*, 6654−6664.
(26) Binks, B. P.; Lumsdon, S. O. *Langmuir* **2000**, *16*, 8622−8631.
(27) Wang, D.; Astruc, D. *Chem. Rev.* **2014**, *114*, 6949−6985.
(28) Ebbens, S.; Jones, R. A. L.; Ryan, A. J.; Golestanian, R.; Howse, J. R. *Phys. Rev. E* **2010**, *82*, 015304.
(29) Schramm, L. L.; Hepler, L. G. *Can. J. Chem.* **1994**, *72*, 1915−1920.
(30) Tsai, S. S. H.; Wexler, J. S.; Wan, J. D.; Stone, H. A. *Lab Chip* **2013**, *13*, 119−125.

DOI: 10.1021/acsami.5b01053
ACS Appl. Mater. Interfaces 2015, 7, 7795−7800